tential energy of the $4f$ electron in the field of dipoles of four fluorines dynamically polarized by the moving point charge of the H^- ion the second-degree terms are as follows:

$$\alpha_0^{(2)} = \frac{\alpha_F eq}{2R^4S^3} r^2 \left\{ \frac{4v}{S^2} \left[4w P_3^1\left(\frac{u}{R}\right) + 3v P_3^0\left(\frac{u}{S}\right) \right] - 24 P_3^0\left(\frac{u}{R}\right) \right\},$$

$$\beta_0^{(2)} = -\frac{2\alpha_F eq}{R^4S^5} r^2 \left\{ \left(\frac{5v^2}{S^2} - 1\right) \left[4w P_3^1\left(\frac{w}{R}\right) + 3v P_3^0\left(\frac{w}{R}\right) \right] - 24 v P_3^0\left(\frac{u}{R}\right) \right\}, \quad \text{(A9)}$$

$$\gamma_0^{(2)} = \frac{\alpha_F eq}{R^4S^5} r^2 \left[8w \left(5\frac{w^2}{S^2} - 3\right) P_3^1\left(\frac{u}{R}\right) + 3v \left(10\frac{w^2}{S^2} - 1\right) P_3^0\left(\frac{u}{R}\right) \right].$$

The meaning of the parameters R, S, D, u, v, and w is indicated in Fig. 1.

*On leave from the Institute of Radio Electronics, Czechoslovak Academy of Science, Prague, Czechoslovakia.

[1]G. D. Jones, S. Peled, R. Rosenwaks, and S. Yatsiv, Phys. Rev. 183, 353 (1969).

[2]H. M. Crosswhite, R. L. Schwiesow, and W. T. Carnall, J. Chem. Phys. 50, 5032(L) (1969).

[3]C. Ryter, Helv. Phys. Acta 30, 353 (1957); W. Low, Phys. Rev. 109, 265 (1958).

[4]J. M. Baker, B. Bleaney, and W. Hayes, Proc. Roy. Soc. (London) A247, 141 (1958); J. Sierro, Helv. Phys. Acta 36, 505 (1963); J. Sierro and R. Lacroix, Compt. Rend. 250, 2686 (1960); V. M. Vinokurov, M. M. Zaripov, Yu. E. Polskii, V. G. Stepanov, G. K. Chirkin, and L. Ya. Shekun, Fiz. Tverd. Tela 4, 2238 (1962) [Soviet Phys. Solid State 4, 1637 (1963)].

[5]J. Sierro, J. Chem. Phys. 34, 2183 (1961); J. Sierro, Helv. Phys. Acta 36, 505 (1963); V. M. Vinokurov, M. M. Zaripov, Yu. E. Polskii, V. G. Stepanov, G. K. Chirkin, and L. Ya. Shekun, Fiz. Tverd. Tela 5, 599 (1963) [Soviet Phys. Solid State 5, 436 (1963)].

[6]K. W. H. Stevens, Proc. Phys. Soc. (London) A65, 209 (1952).

[7]M. T. Hutchings, in *Solid State Physics*, Vol. 16, edited by F. Seitz and D. Turnbull (Academic, New York, 1964).

[8]V. M. Vinokurov, M. M. Zaripov, Yu. E. Polskii, V. G. Stepanov, G. K. Chirkin, and L. Ya. Shekun, Fiz. Tverd. Tela 5, 2902 (1963) [Soviet Phys. Solid State 5, 2126 (1964)].

[9]B. G. Wybourne, Phys. Rev. 148, 317 (1966).

[10]B. G. Wybourne, *Spectroscopic Properties of Rare Earths* (Wiley, New York, 1965).

[11]W. T. Carnall (unpublished results communicated by B. G. Wybourne).

[12]S. Fraga and G. Malli, *Many-Electron Systems: Properties and Interactions* (Saunders, Philadelphia, 1968), p. 89.

[13]I. T. Jacobs, G. D. Jones, K. Ždánský, and R. A. Satten, Phys. Rev. B (to be published).

[14]D. Kiro and W. Low, Phys. Letters 29A, 537 (1969).

[15]The sign of the contribution depends on the relative values of the radial w_x and axial w_z frequencies of the H^- local mode. Originally it was thought that $w_x > w_z$ (Ref. 1), but now it has been proved that $w_x < w_z$ (Ref. 13).

PHYSICAL REVIEW B VOLUME 3, NUMBER 7 1 APRIL 1971

Hyperfine, Superhyperfine, and Quadrupole Interactions of Gd^{3+} in YPO_4

J. C. Danner, U. Ranon,* and D. N. Stamires

Douglas Advanced Research Laboratories, McDonnell Douglas Corporation, Huntington Beach, California 92647

(Received 27 February 1970)

The electron-paramagnetic-resonance spectrum of Gd^{3+} in YPO_4 shows a superhyperfine structure from two nearest-neighbor phosphorus nuclei when observed with $\vec{H}$ parallel to the crystal c axis. The spectrum for $\vec{H}$ perpendicular to the c axis is unusual because of quadrupole interactions in Gd^{155} and Gd^{157} which are larger than the hyperfine interaction in these ions. The measured Gd^{3+}-P interaction parameter $|T_{\parallel}| = 1.02$ G fits well a dipole-dipole interaction model. The hyperfine parameters are $A^{155} = -4.7$ G and $A^{157} = -6.1$ G. The quadrupole-interaction parameters are $|Q^{155}| = 18.1$ G and $|Q^{157}| = 19.3$ G. From these the ratio of the nuclear quadrupole moments of Gd^{155} and Gd^{157} is obtained as 0.94 ± 0.01. This result is discussed in the light of quadrupole moments previously measured by optical and nuclear methods.

I. INTRODUCTION

Paramagnetic resonance of Gd^{3+} in YPO_4 has been recently observed by several authors.[1-3] Variable-frequency zero-field EPR[1,2] and conventional EPR[3] were used to determine the magnitude and sign[3] of the crystal-field parameters b_n^m. These parameters[4] describe the splitting of the $^8S_{7/2}$ ground

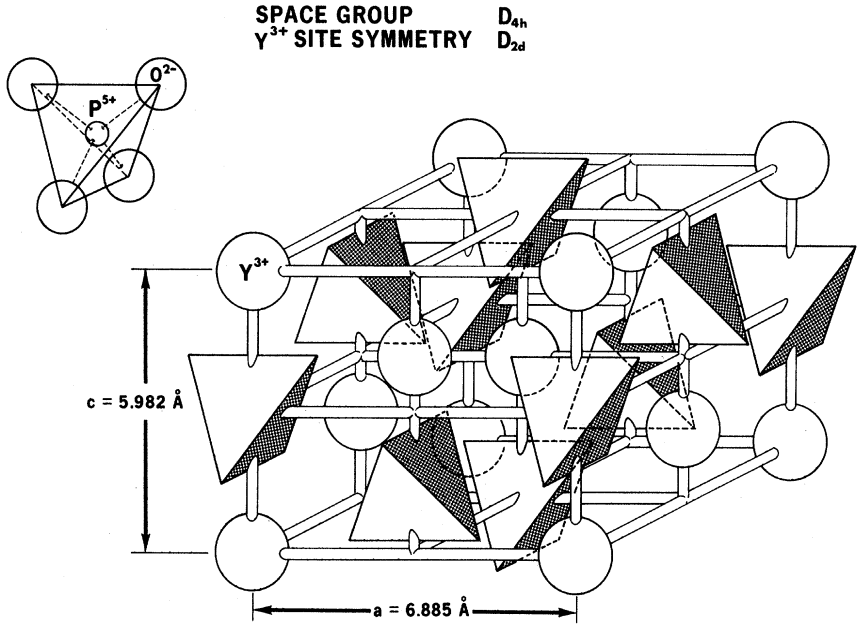

FIG. 1. Structure of YPO_4.

state of Gd^{3+} in the crystal field of YPO_4.

In the EPR experiments reported so far on Gd^{3+} in YPO_4, no hyperfine structure was observed. In the present work we wish to report the observation of hyperfine structure of Gd^{155} and Gd^{157} and of superhyperfine structure due to interaction with two nearest-neighbor P nuclei in the YPO_4 lattice. In addition, it was found that the nuclear quadrupole interaction of the odd isotopes is larger than the hyperfine interaction. This is a rather uncommon case and gives rise to an unusual spectrum. It makes possible an accurate determination of the nuclear quadrupole-interaction parameter Q of both odd isotopes. Furthermore, an accurate ratio of their nuclear quadrupole moments can be obtained.

Naturally occurring gadolinium is composed of 70% even isotopes and 30% odd isotopes. The main stable odd isotopes are Gd^{155} and Gd^{157}, which have almost equal abundance. Each of the odd isotopes has a nuclear spin $I = \frac{3}{2}$. Hyperfine structure from the odd isotopes is not always resolved in EPR experiments, because the splitting is small[5] (of the order of 5×10^{-4} cm^{-1}) and is sometimes obscured by the width of the even-isotope lines. The intensity ratio between a hyperfine line and the even-isotope line (for the same electronic transition) is approximately 1 : 20.

The crystal structure of YPO_4 is described in Sec. II, followed by a presentation of the appropriate spin Hamiltonian. Experimental results are given in Sec. IV and are discussed in Sec. V.

II. CRYSTAL STRUCTURE

YPO_4 has the zircon structure which is shown in Fig. 1. The cell parameters are taken from Wyckoff.[6] The structure belongs to space group D_{4h} and the yttrium site has D_{2d} point symmetry. Rare-earth ions substitute for Y^{3+} at this site. There are four such sites in the unit cell but magnetically they are all equivalent. The main rotation axis of the point symmetry is parallel to the crystal c axis so that the principal axis of the spin Hamiltonian can be taken along this direction.

Since we will be interested in the interaction between the Gd^{3+} ions and neighboring phosphorus nuclei, Fig. 2 shows the position of first-, second-, and third-nearest-neighbor P ions in relation to the Gd^{3+} ion. The two nearest-neighbor phosphorus ions are located at a distance $r_1 = 2.99$ Å, one on

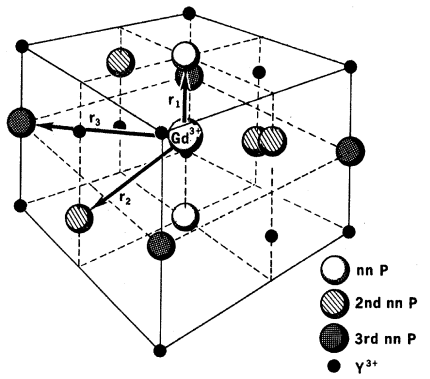

FIG. 2. Location of first-, second-, and third-nearest-neighbor P atoms in relation to a Gd^{3+} ion at a Y^{3+} lattice site in YPO_4. The vectors r_1, r_2, and r_3 show the relative position of these neighbors. The magnitudes of the vectors are $|r_1| = 2.99$ Å, $|r_2| = 4.85$ Å, $|r_3| = 4.85$ Å.

each side of the Gd^{3+} ion, along the c axis. In the absence of oxygens, the two phosphorus ions are related by inversion through the Gd^{3+} position. Therefore, they are equivalent as far as the direct interaction with the Gd^{3+} ion is concerned. The four second-nearest phosphorus nuclei are at a distance $r_2 = 3.75$ Å from the Gd^{3+} ion along the directions [201], [$\bar{2}$01], [0$\bar{2}$1], and [02$\bar{1}$]. The radius vector $\vec{r}_2$ is at an angle θ_2 to the c plane such that $\cos\theta_2 = 0.918$. The four third neighbors are at a distance $r_3 = 4.85$ Å from the Gd^{3+} ion along ⟨110⟩ and its equivalent directions.

III. THEORY

In this section we first describe the spin Hamiltonian appropriate to our case. Next the evaluation of the eigenvalues and transition is divided into three parts. The splitting of the $S=\frac{7}{2}$ state is discussed first. Then eigenvalues and transitions of the $S_z = \pm\frac{1}{2}$ doublet are calculated for $\vec{H}$ along the c axis, taking into consideration both hyperfine and superhyperfine terms. Finally, eigenvalues and transitions of the $S_z = \pm\frac{1}{2}$ doublet are calculated for $\vec{H}$ perpendicular to c assuming $|Q| > |A|$. The calculations were limited to these cases in light of the experimental results which are presented in Sec. IV. No quadrupole effects are observed when $\vec{H}$ is parallel to c, while no superhyperfine structure is observed when $\vec{H}$ is perpendicular to c.

A. Spin Hamiltonian

In order to describe the experimental spectrum, the spin Hamiltonian[5] has to be written in a form which reflects the local symmetry at the Gd^{3+} site and include the various interactions both within the ion and between the ion and its neighbors. Accordingly, we write for the spin Hamiltonian

$$\mathcal{H} = \mathcal{H}_c + \mathcal{H}_Z + \mathcal{H}_{hf} + \mathcal{H}_P \,. \tag{1}$$

$\mathcal{H}_c$ represents the crystal-field interaction which in YPO_4 splits the $J=S=\frac{7}{2}$ ground state of Gd^{3+} into four close doublets. It has the form

$$\mathcal{H}_c = b_2^0 O_2^0 + b_4^0 O_4^0 + b_6^0 O_6^0 + b_4^4 O_4^4 + b_6^4 O_6^4 \,, \tag{2}$$

where b_2^0 are crystal-field parameters[4,7] and O_n^m are operator equivalents.[7] The crystal-field parameters for YPO_4; Gd^{3+} have been reported.[2,3] The predominant term in (2) is $b_2^0 = -0.0728$ cm^{-1} (at room temperature[3]), which is between one and three orders of magnitude larger than any other of the b_n^m's. This gives the local crystal field an almost purely axial character.

The second term in (1), $\mathcal{H}_Z$, is the Zeeman interaction with the external magnetic field. Usually only the electronic part of this interaction is retained since the nuclear Zeeman interaction for both the odd gadolinium isotopes and the phosphorus nuclei is comparatively small. Also, it does not shift the ordinary EPR transition in which the nuclear-spin quantum number m does not change. However, in the present case we shall see that the nuclear Zeeman term is not negligible and therefore is included in $\mathcal{H}_Z$.

The Zeeman term in this symmetry is[5]

$$\mathcal{H}_Z = g_\parallel \mu_B H_z S_z + g_\perp \mu_B (H_x S_x + H_y S_y) - \gamma_N \vec{H}\cdot\vec{I} \,, \tag{3}$$

where $S=\frac{7}{2}$ is the true spin of Gd^{3+} in its ground state, $\vec{H}$ is the magnetic field, μ_B is the Bohr magneton, $g_\parallel$ and $g_\perp$ are the principal values of the g tensor in the local crystal-field coordinate system, and γ_N is the nuclear magnetogyric ratio. In S-state ions, the electronic distribution is spherically symmetric. Therefore, if the crystal-field splitting is not much larger than the Zeeman splitting, the g tensor tends to be isotropic so that $g_\parallel = g_\perp$. This is the case here too with[3] $g_\parallel = 1.991$.

$\mathcal{H}_{hf}$ in (1) represents the hyperfine and quadrupole interaction for the odd Gd^{3+} isotopes. It has the form[5]

$$\mathcal{H}_{hf} = AS_zI_z + B(S_xI_x + S_yI_y) + Q[I_z^2 - \tfrac{1}{3}I(I+1)] \,, \tag{4}$$

which reflects the site symmetry. Because g is isotropic, $A=B$ and $\mathcal{H}_{hf}$ has the form

$$\mathcal{H}_{hf} = A\vec{S}\cdot\vec{I} + Q[I_z^2 - \tfrac{1}{3}I(I+1)] \,, \tag{5}$$

where the second term represents the quadrupole interaction.

The last term in (1), $\mathcal{H}_P$, represents the superhyperfine interaction with the phosphorus nuclei. It can be written in the form[8]

$$\mathcal{H}_P = \sum_i \vec{S}\cdot\overleftrightarrow{T}_i\cdot\vec{I}_i^P \,, \tag{6}$$

where the summation is over all the interacting phosphorus nuclei. It is assumed that the phosphorus nuclei do not interact with each other. $\overleftrightarrow{T}_i$ is the superhyperfine interaction tensor between the nucleus of the phosphorus ion P_i with nuclear spin I_i^P and the Gd^{3+}. $\overleftrightarrow{T}_i$ will have a different form for each of the groups of P nuclei shown in Fig. 2. We shall be mainly interested in the two nearest neighbors, and for these the principal axes of $\overleftrightarrow{T}_i$ coincide with those of the local crystal field. Furthermore, the symmetry at these nuclei is axial. Therefore, for these nuclei (6) can be written in the same coordinate system as (3) and (4) in the form

$$\mathcal{H}_P = 2\vec{S}\cdot\overleftrightarrow{T}\cdot\vec{I}^P = 2[T_\parallel S_z I_z^P + T_\perp (S_x^P I_x^P + S_y^P I_y^P)] \,, \tag{7}$$

where the subindex i is omitted; $T_\parallel$ and $T_\perp$ are the principal values of this interaction tensor and a factor of 2 is included because two equivalent P nuclei are involved.

B. Energy Levels and Transitions

1. *Splitting of $S=\frac{7}{2}$ State in an Axial Field*

The splitting of an $S=\frac{7}{2}$ state by a crystal field has been widely discussed in the literature.[3,5,9] In the present case, where the term $b_2^0 O_2^0$ is the predominant crystal-field interaction, the $S=\frac{7}{2}$ state is split into four doublets with eigenfunctions $|\pm S_z\rangle$. The separation between the doublets is

$$|\pm(M+1)\rangle - |\pm M\rangle = (2M+1)b_2^0$$

for $M=\frac{1}{2}, \frac{3}{2}$, and $\frac{5}{2}$, respectively.

The usual magnetic-dipole EPR transitions are $\Delta M=\pm 1$. With the external field oriented parallel to the c axis, the spectrum consists of seven electronic transitions separated by $2b_2^0$ from each other. Small shifts from this even separation are caused by other terms of $\mathcal{H}_c$.

The position of the $|\frac{1}{2}\rangle \rightarrow |-\frac{1}{2}\rangle$ transition is not affected by the crystal field in first order, because it is the only transition in the spectrum within a Kramers doublet. Therefore its line shape and linewidth will be the least affected by crystal strains and irregularities of the crystal field. It is thus the best transition for observation of weak hyperfine, superhyperfine, and other interactions. Indeed, the lines due to interaction with neighboring P nuclei, as well as the hyperfine lines of Gd^{155} and Gd^{157}, were best resolved on it. For this reason we confine our analysis to this transition.

2. *Eigenvalues and Transitions for $S_z=\pm\frac{1}{2}$ Doublet With Hyperfine and Superfine Interaction, $\vec{H}\parallel c$*

The spin Hamiltonian is now

$$\mathcal{H}=g_{\parallel}\mu_B H S_z + A\vec{S}\cdot\vec{I} + Q[I_z^2 - \tfrac{1}{3}I(I+1)] - \gamma_N \vec{H}\cdot\vec{I} + 2\textstyle\sum_i \vec{S}\cdot\vec{T}_i\cdot\vec{I}_i^{\,P}. \quad (8)$$

In the present case the quadrupole and nuclear Zeeman terms can be omitted. Since A is very small in gadolinium, there is negligible admixture between the nuclear states by the hyperfine term in (8). Therefore, the EPR transitions will be of the $\Delta m = 0$ type, and they are not affected here by either of these two terms.

The last term in (8) has the axial form given in (7) and describes the interaction with the two closest P ions. The role of the more distant P ions is discussed in Sec. V.

If it is also assumed that $|T_{\parallel}|$, $|T_{\perp}| \ll H$, the term in $T_{\perp}$ can be neglected and (8) will have the form

$$\mathcal{H}=(g\mu_B H + AI_z + T_{\parallel}I_{z,1}^P + T_{\parallel}I_{z,2}^P)S_z\,, \quad (9)$$

where the last two terms stand for the two nearest-neighbor P nuclei.

The energy levels of (9) can be obtained by inspection:

$$E(\pm\tfrac{1}{2}, m, m_1^P, m_2^P) = \tfrac{1}{2}[g\mu_B H + Am + T_{\parallel}(m_1^P + m_2^P)]\,, \quad (10)$$

and the EPR transitions are

$$h\nu = g\mu_B H + Am + T_{\parallel}(m_1^P + m_2^P)\,. \quad (11)$$

If $|T_{\parallel}| < |A|$, the superhyperfine interaction will give rise to a structure on the hyperfine lines of Gd^{155} and Gd^{157}. Since $I^P=\frac{1}{2}$, $m_1^P, m_2^P=\pm\frac{1}{2}$ and the superhyperfine term will cause a splitting $T_{\parallel}$ between superhyperfine lines. The eigenvalues of $m_1^P+m_2^P$ are 1, 0, 0, -1, so that each pair of nearest-neighbor P nuclei should give rise to a triplet of superhyperfine lines with an intensity ratio 1:2:1.

3. *Eigenvalues and Transitions for $S_z=\pm\frac{1}{2}$ Doublet With Hyperfine Interaction, $|A| < |Q|$, $\vec{H}\perp c$*

The spin Hamiltonian is

$$\mathcal{H}=\mathcal{H}_Z+\mathcal{H}_{hf}\,, \quad (12)$$

with the magnetic field perpendicular to the crystal c axis. For the purpose of calculating eigenvalues of (12) it is most convenient to transform the spin Hamiltonian into a coordinate system where the direction of $\vec{H}$ is the quantization axis. This transformation has been treated by Bleaney.[5,10] Applying the transformation to the present case, the spin Hamiltonian (12) is

$$\mathcal{H}=g\mu_B H S_z + AS_z I_z + \tfrac{1}{2}A(S_+I_- + S_-I_+) - \tfrac{1}{2}Q[I_z^2 - \tfrac{1}{3}I(I+1)] + \tfrac{1}{4}Q[I_+^2 + I_-^2] - \gamma_N H I_z\,. \quad (13)$$

Here $S_{\pm}$ and $I_{\pm}$ are the operators $S_x \pm iS_y$ and $I_x \pm iI_y$, respectively.

The off-diagonal term in A can be neglected since $A \ll g\mu_B H$. But now the nuclear states are admixed by the quadrupole term, and the admixture depends on the ratio Q/A. Bleaney[10] has calculated the eigenvalues of (13) for $A \gg Q$ in a general case. We are interested, however, in calculating the eigenvalues when $Q > A$. This is easily done for $S=\frac{1}{2}$ and the neglect of the off-diagonal elements of A. The 4×4 matrices for $S_z=\frac{1}{2}$ and $S_z=-\frac{1}{2}$ are reduced to 2×2 matrices connecting nuclear states $(m, m-2)$. The secular equations for $S_z=\pm\frac{1}{2}$ are

$$\begin{vmatrix} \pm g\mu_B H + \frac{3}{2}A - Q - 3\gamma_N H - 2E & \sqrt{3}\,Q \\ \sqrt{3}\,Q & \pm g\mu_B H \mp \frac{1}{2}A + Q + \gamma_N H - 2E \end{vmatrix} = 0 \qquad \text{for } (m, m-2) = (\tfrac{3}{2}; -\tfrac{1}{2}) \quad (14)$$

and

$$\begin{vmatrix} \pm g\mu_B H \pm \tfrac{1}{2}A + Q - \gamma_N H - 2E & \sqrt{3}\,Q \\ \sqrt{3}\,Q & \pm g\mu_B H \mp \tfrac{3}{2}A - Q + 3\gamma_N H - 2E \end{vmatrix} = 0 \quad \text{for } (m, m-2) = (\tfrac{1}{2}, -\tfrac{3}{2}). \tag{15}$$

From (14) and (15) the energy levels can be calculated assuming $Q > A$. If terms up to the order A^3/Q^3 are retained, the energy levels for $S_z = \pm\frac{1}{2}$ are

$$\begin{aligned} E_1(\pm) &= \pm\tfrac{1}{2}g\mu_B H + Q + \xi(\mp) + \eta(\mp), \\ E_2(\pm) &= \pm\tfrac{1}{2}g\mu_B H + Q\,\xi(\mp) - \eta(\mp), \\ E_3(\pm) &= \pm\tfrac{1}{2}g\mu_B H - Q + \tfrac{1}{2}(A \mp \gamma_N H) - \xi(\mp) - \eta(\mp), \\ E_4(\pm) &= \pm\tfrac{1}{2}g\mu_B H - Q - \tfrac{1}{2}(A \mp \gamma_N H) - \xi(\mp) + \eta(\mp), \end{aligned} \tag{16}$$

where

$$\xi(\mp) = 3(A \mp 2\gamma_N H)^2/8Q, \tag{17}$$

$$\eta(\mp) = 3(A \mp 2\gamma_N H)^3/128Q^2. \tag{18}$$

The energy levels of (16) are plotted in Fig. 3 assuming $Q > 0$.

In order to calculate transition probabilities, the eigenfunctions of the $E_i(\pm)$ states are required. These are easily obtained from (14) and (15). The eigenfunctions are given as combinations of the four nuclear states $|\pm\frac{3}{2}\rangle$ and $|\pm\frac{1}{2}\rangle$ in the two electronic states $S_z = +\frac{1}{2}$ and $S_z = -\frac{1}{2}$, and are designated $\psi(+)$ and $\psi(-)$, respectively.

We get

$$\begin{aligned} \psi_1(\pm) &= \cos\phi(\pm)\,|\pm\tfrac{3}{2}\rangle + \sin\phi(\pm)\,|\mp\tfrac{1}{2}\rangle, \\ \psi_2(\pm) &= \cos\theta(\pm)\,|\pm\tfrac{1}{2}\rangle + \sin\theta(\pm)\,|\mp\tfrac{3}{2}\rangle, \\ \psi_3(\pm) &= -\sin\phi(\pm)\,|\pm\tfrac{3}{2}\rangle + \cos\phi(\pm)\,|\mp\tfrac{1}{2}\rangle, \\ \psi_4(\pm) &= -\sin\theta(\pm)\,|\pm\tfrac{1}{2}\rangle + \cos\theta(\pm)\,|\mp\tfrac{3}{2}\rangle, \end{aligned} \tag{19}$$

where

$$\cos\phi(+) = Q/\{3[Q - (\tfrac{1}{2}A - \gamma_N H)]^2 + Q^2\}^{1/2},$$

$$\sin\phi(-) = \sqrt{3}\,Q/\{[Q + (\tfrac{1}{2}A + \gamma_N H)]^2 + 3Q^2\}^{1/2},$$

and

$$\begin{aligned} \cos\theta(+) &= \sqrt{3}\,Q/\{[Q - (\tfrac{1}{2}A - \gamma_N H)]^2 + 3Q^2\}^{1/2}, \\ \sin\theta(-) &= Q/\{3[Q + (\tfrac{1}{2}A + \gamma_N H)]^2 + Q^2\}^{1/2}. \end{aligned} \tag{20}$$

In calculating transition probabilities we have omitted the nuclear Zeeman term $\gamma_N H$ because, within the experimental accuracy, its contribution to the line intensity is negligible.

From the matrices of (14) and (15) and from (20) we have calculated the position and intensities of the various $\Delta M = 1$ transitions as a function of the ratio Q/A. In Fig. 4(a) the separation ΔH of the lines from the even-isotope line (at $\Delta H = 0$) is plotted in units of A. In Fig. 4(b) the relative intensities of the lines are plotted as a function of Q/A.

The transitions fall into two groups. These are indicated by the solid and broken lines in Fig. 4. We shall refer to these as group (a) and group (f), respectively. Group (a), which has maximum intensity for $Q = 0$, corresponds to the so-called "allowed" ($\Delta m = 0$) transitions in EPR. As the quadrupole interaction increases, group (f), which corresponds to the so-called "forbidden" ($\Delta m = 2$) transitions, gains in intensity while the intensity of group (a) decreases. At the same time, the lines of group (a) move sharply away from the even-isotope lines, as seen in Fig. 4(a). For $|Q/A| = 0.5$, the intensities of the two groups are

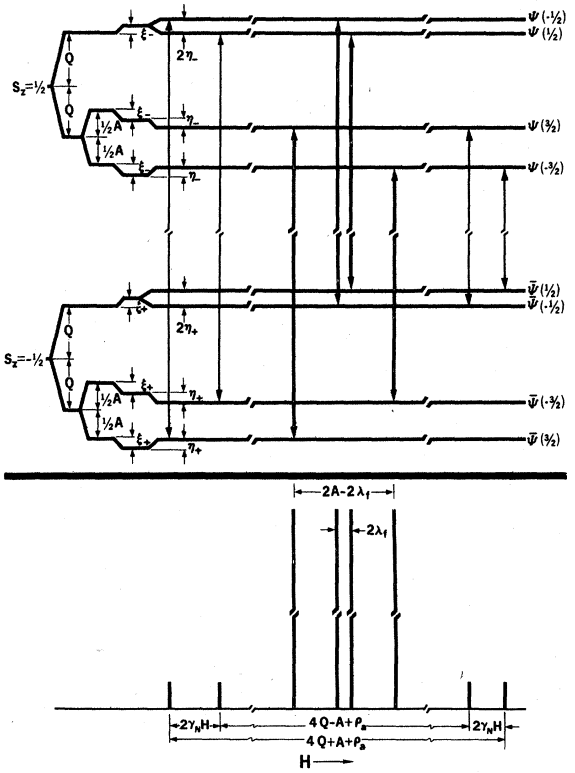

FIG. 3. Energy levels and transitions of the spin Hamiltonian (13); $H \perp c$, assuming $Q > A$; $S = \frac{1}{2}$, $I = \frac{3}{2}$. Splittings by successively smaller terms are shown from left to right. Splittings are not to scale. Intense and weak transitions are shown by thick and thin arrows, respectively. A schematic spectrum showing the various splittings is given at the bottom of the figure. The parameters and eigenfunctions are discussed in the text.

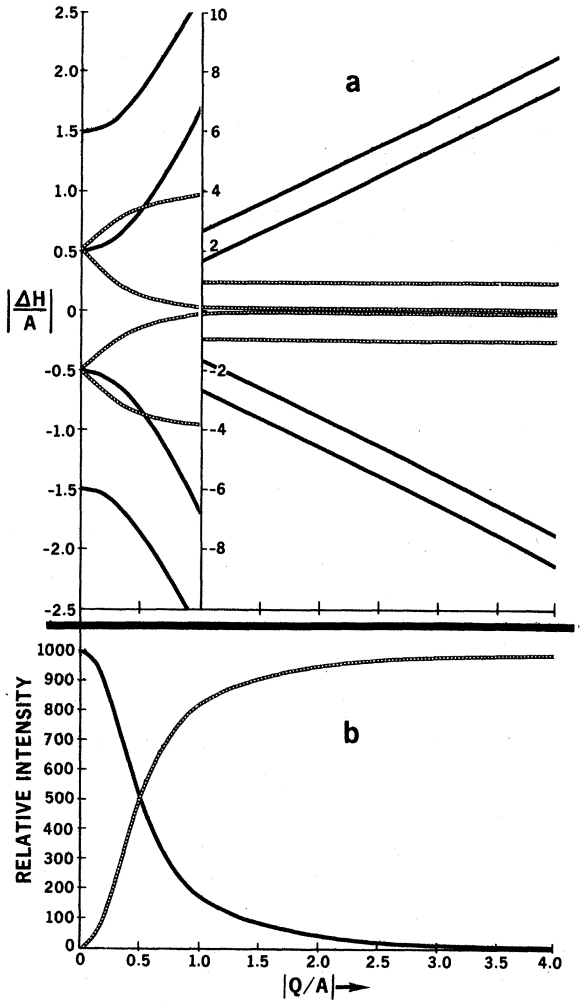

FIG. 4. (a) EPR spectrum described by spin Hamiltonian (13); $H \perp c$, with $S=\frac{1}{2}$, $I=\frac{3}{2}$ showing the position of lines in terms of the parameter $|A|$ as a function of $|Q/A|$. Note change of scale for $|Q/A|>1$. (b) Relative intensities of the two groups of lines in (a) as a function of $|Q/A|$. The solid and broken curves indicate the normal hyperfine lines and the quadrupole-induced lines. They correspond to group (a) and group (f) in the text, respectively.

already equal and there is really no meaning to the terms "allowed" and "forbidden" transitions. For $|Q| > 0.5|A|$ the forbidden lines become allowed and vice versa. It is interesting to note that the outermost lines in group (f) approach asymptotically an over-all splitting of $2A$ as $|Q/A|$ increases.

The transitions in group (a) are

$$\begin{aligned} a_1&: h\nu = g\mu_B H + 2Q + (\tfrac{1}{2}A + \gamma_N H) + \rho_a + \lambda_a , \\ a_2&: h\nu = g\mu_B H + 2Q - (\tfrac{1}{2}A + \gamma_N H) + \rho_a - \lambda_a , \\ a_3&: h\nu = g\mu_B H - 2Q + (\tfrac{1}{2}A - \gamma_N H) - \rho_a - \lambda_a , \end{aligned} \tag{21}$$

$$a_4: h\nu = g\mu_B H - 2Q - (\tfrac{1}{2}A - \gamma_N H) - \rho_a + \lambda_a ,$$

where

$$\rho_a = \xi(+) + \xi(-) , \quad \lambda_a = \eta(-) - \eta(+) .$$

The transitions in group (f) are

$$\begin{aligned} f_1&: h\nu = g\mu_B H + A - \rho_f - \lambda_f , \\ f_2&: h\nu = g\mu_B H + \rho_f + \lambda_f , \\ f_3&: h\nu = g\mu_B H + \rho_f - \lambda_f , \\ f_4&: h\nu = g\mu_B H - A - \rho_f + \lambda_f , \end{aligned} \tag{22}$$

where

$$\rho_f = \xi(-) - \xi(+), \quad \lambda_f = \eta(+) + \eta(-) ,$$

and $h\nu$ is the microwave quantum energy. From the *field* separation of different lines the various spin-Hamiltonian parameters can be determined. For example,

$$\begin{aligned} a_4 - a_1 &= 4Q + A + 2\rho_a , \\ a_3 - a_2 &= 4Q - A + 2\rho_a , \\ a_4 - a_3 &= A - 2\gamma_N H - 2\lambda_a , \\ a_2 - a_1 &= A + 2\gamma_N H + 2\lambda_a , \end{aligned} \tag{23}$$

$$\begin{aligned} f_4 - f_1 &= 2A - 2\lambda_f , \\ f_3 - f_2 &= 2\lambda_f . \end{aligned} \tag{24}$$

The transition groups (a) and (f) and the separation (23) and (24) are also shown in Fig. 3, where λ_a was neglected.

IV. EXPERIMENT AND RESULTS

The experiments were done on a Varian EPR spectrometer operating at K_a band. Most of the data was taken at room temperature. A few runs were done at 4.2 and 1.4 °K. No major differences in the spectrum were found by going from room temperature to the low temperatures.

As stated earlier, the $|\frac{1}{2}\rangle \rightarrow |-\frac{1}{2}\rangle$ electronic transition was the one studied in detail. The observed spectrum of this transition for H along the c axis is shown at the bottom of Fig. 5. The way this spectrum is constructed from the hyperfine splitting of Gd^{155} and Gd^{157} and the superhyperfine interaction with the two nearest-neighbor P nuclei is shown at the top of Fig. 5. From the spectrum and from Eq. (11) we get

$$A^{157} = -6.1 \text{ G} ,$$

$$A^{155} = -4.7 \text{ G} ,$$

$$|T_{\parallel}| = 1.02 \pm 0.03 \text{ G} .$$

In the spectrum of the $|\frac{1}{2}\rangle \rightarrow |-\frac{1}{2}\rangle$ electronic transition, for H perpendicular to the c axis, no

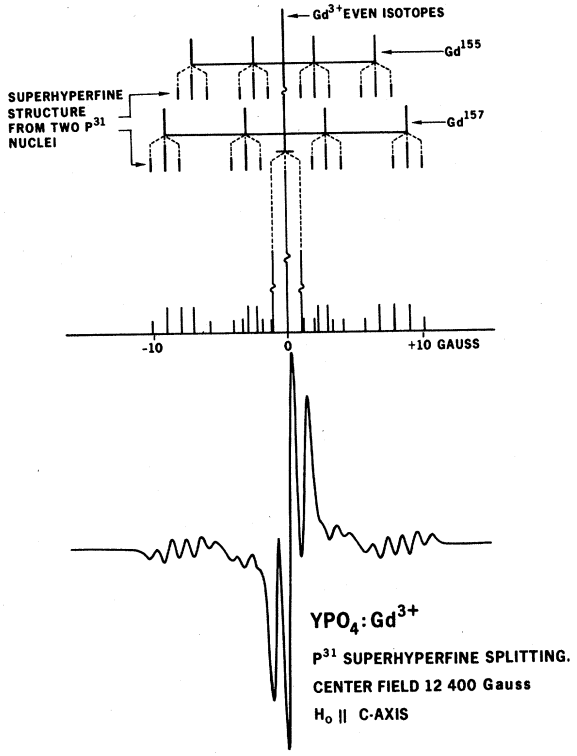

FIG. 5. EPR spectrum of Gd^{3+} in YPO_4 at K_a band with H parallel to c showing the superhyperfine splitting from adjacent P nuclei.

superhyperfine structure is observed. The spectrum is shown at the top of Fig. 6. At the bottom of this figure, bar spectra are shown for the two isotopes 155 and 157. The lines for each isotope correspond to the transitions shown in Fig. 3. The center two lines of Fig. 3 are masked in the actual spectrum by the even-isotope line, and therefore are not shown in the bar spectra.

From the spectrum and the various expressions in Sec. III B, we obtained values for Q and A. The nuclear Zeeman contribution was calculated from the nuclear magnetic moments of Gd^{155} and Gd^{157} determined by Baker *et al.*[11] and the sign of the A parameters taken from their results.

The parameters A and Q are given in Table I. From the results we obtain $|Q/A|^{155} = 3.9$, $|Q/A|^{157} = 3.2$, and eigenfunction coefficients which are given in Table II.

TABLE I. Spin-Hamiltonian parameters for Gd^{+3} in YPO_4, $g_{\parallel} = 1.991$.

	A^{155}	A^{157}	$\lvert Q^{155}\rvert$	$\lvert Q^{157}\rvert$	$T_{\parallel}$
G	-4.67	-6.09	18.1	19.3	1.02
	±0.03	±0.03	±0.1	±0.1	±0.03
10^{-4} cm^{-1}	-4.34	-5.66	16.8	17.9	0.95
	±0.03	±0.03	±0.1	±0.1	±0.03

TABLE II. Eigenfunction coefficients for Gd^{155} and Gd^{157} in YPO_4.

	$\cos\phi(\pm)$	$\sin\phi(\pm)$	$\cos\theta(\pm)$	$\sin\theta(\pm)$
		Gd^{155}		
(+)	0.552	0.834	0.893	0.450
(-)	0.545	0.838	0.889	0.457
		Gd^{157}		
(+)	0.564	0.826	0.899	0.439
(-)	0.555	0.832	0.895	0.447

The relative intensity of the observed lines in groups (a) and (f) is in good agreement with the theory. From the eigenfunctions we get, for the relative intensity $R = (f)/(a)$, $R^{155} = 99:1.2$ and $R^{157} = 98:2$. It is difficult to compare the intensities of the (f) lines, but one can compare the intensities of the weak (a) lines of both isotopes. Since the Gd^{155} and Gd^{157} isotopes are of almost equal abundance and have the same nuclear spin, the R numbers represent the actual intensities. As can be seen from Fig. 4 and the calculated R values, it is very sensitive to the value of $|Q/A|$. Therefore, $(a)^{155}/(a)^{157}$ is also sensitive to this value, and can serve as a good test of the theory. Com-

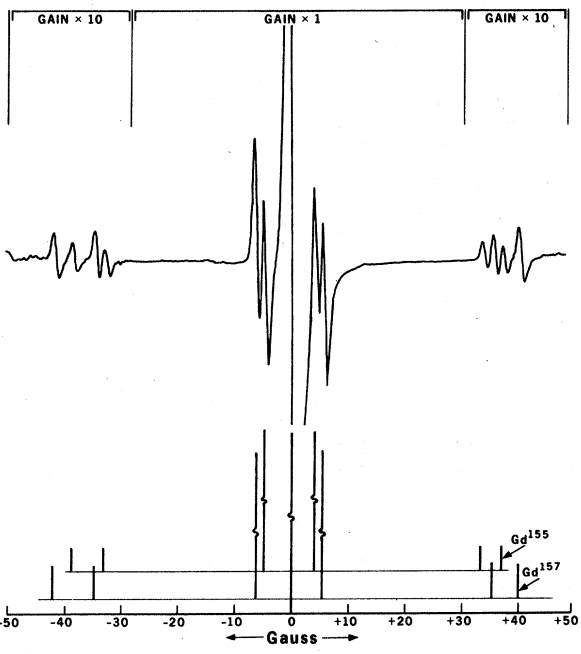

FIG. 6. EPR spectrum of the $|\frac{1}{2}\rangle \rightarrow |-\frac{1}{2}\rangle$ transition of Gd^{3+} in YPO_4 at 35 GHz and room temperature measured with the magnetic field perpendicular to the crystal c axis. Note change in instrument gain for weak lines.

parison of the (a) lines in Fig. 6 with the calculated ratio $(a)^{155}/(a)^{157} = 0.6$ shows rather good agreement.

V. DISCUSSION

A. Superhyperfine Interaction

The observation of superhyperfine splitting from the nearest-neighbor P nuclei when H is along the c axis, and the absence of such splitting in the perpendicular plane, requires a closer investigation of the P-Gd interaction.

Assuming a dipole-dipole interaction between the phosphorus nuclei and the gadolinium electrons, the magnetic field due to a P nucleus at the Gd site is given by

$$(\mu_P/r^3)(3\cos^2\theta - 1), \tag{25}$$

where μ_P is the phosphorus nuclear magnetic moment, r is the P-Gd separation, and θ is the angle between the direction of the field H and the P-Gd radius vector. The nuclear magnetic moment of ^{31}P is $+1.1566\mu_N$.[12] The distances r_i of the first-, second-, and third-nearest-neighbor P ions are, respectively,[6] $r_1 = 2.99$ Å, $r_2 = 3.75$ Å, and $r_3 = 4.85$ Å. We have then

$$\mu_P/r_1^3 = 0.25 \text{ G},$$

$$\mu_P/r_2^3 = 0.13 \text{ G},$$

and

$$\mu_P/r_3^3 = 0.06 \text{ G}.$$

When the external magnetic field H is along c, the angles θ are such that $\cos^2\theta_1 = 1$, $\cos^2\theta_2 = 0.16$, and $\cos^2\theta_3 = 0$. The magnitude of the field at the Gd site due to each P nucleus is thus

$$h_1 = 0.5 \text{ G}, \quad h_2 = 0.07 \text{ G}, \quad h_3 = 0.06 \text{ G}.$$

The field from the nearest-neighbor P nuclei is seen to be one order of magnitude larger than that from the more distant neighbors.

There are two equivalent nearest-neighbor P nuclei, and therefore their h_1 contributions add algebraically, giving a total field of 1, 0, or -1 G at the Gd. These should be the separations $T_{\parallel}$ of the superhyperfine lines from the hyperfine lines and they are seen to be in excellent agreement with the experimental results.

The hyperfine parameter T also includes a term due to contact interaction between the Gd electrons and the P nucleus. This term is

$$a_s = \tfrac{16}{3}\pi\gamma_N\mu_B\,|\psi(P)|^2, \tag{26}$$

where $|\psi(P)|^2$ is the density of the Gd $4f$ electrons at the P nucleus.

From the data of Freeman and Watson,[13] this contribution amounts to less than 50 mG.

When the magnetic field H is in a perpendicular plane, $\cos^2\theta_1 = 0$ and $h = -0.25$ G. The four second-nearest-neighbor P nuclei act now as two equivalent pairs. If the field H is along [100] or [010], $\cos^2\theta_2 = 0.84$, $h_2 = 0.2$ G and $\cos^2\theta_2 = 0$, $h_2 = -0.13$ G, respectively, for each of the pairs. Along these directions the four third-nearest-neighbor P nuclei are all equivalent with $\cos^2\theta_3 = 0.5$ and $h_3 = 0.03$ G. If $\vec{H}$ is oriented along [110], all four second-nearest neighbors are equivalent, with $\cos^2\theta_2 = 0.42$ and $h_2 = 0.03$ G. The third-nearest neighbors act like two pairs with $\cos^2\theta_3 = 0$ and $h_3 = 0.06$ G, respectively.

The only significant contribution to the superhyperfine structure for H perpendicular to c could thus come from the first and second neighbors. The maximum possible splitting for either group should still be half (or less) than that along c. The EPR lines observed with H perpendicular to c are much broader than those for H along c. This broadening is mainly because of large second-order crystal-field shifts, and it easily obscures any small superhyperfine structure.

B. Quadrupole Interaction

The quadrupole-interaction parameter Q is related to the nuclear quadrupole moment Q_0 by the relation[10]

$$Q = 3eQ_0q/4I(2I-1), \tag{27}$$

where e is the electron charge and q is the gradient of the electric field at the nucleus.

The determination of the parameter Q is done in the present case for two isotopes of equal nuclear spin I, in the same host lattice and the same oxidation state. Therefore, it is safe to assume that q is the same for both isotopes. With this assumption, we have

$$\left|{}^{155}Q/{}^{157}Q\right| = \left|{}^{155}Q_0/{}^{157}Q_0\right| = 0.94 \pm 0.01. \tag{28}$$

The quadrupole moments of the odd Gd isotopes were previously reported by Speck[14] and by Kaliteevskii *et al.*[15] Both obtained the data from optical measurements. Speck gives the values $^{155}Q_0 = 1.1$ b and $^{157}Q_0 = 1.0$ b with an accuracy of 30%. Our results indicate though that $^{157}Q_0 > {}^{155}Q_0$.

The work of Kaliteevskii *et al.* gives a ratio $^{155}Q_0/{}^{157}Q_0 = 0.78 \pm 0.06$, which does not agree with our result.

In general, the determination of interaction parameters such as A and Q from EPR spectra is much more accurate than that from optical data. For one thing, the resolution in EPR spectroscopy is much greater. Also, the approximations involved in describing the one Stark-level cluster in which EPR is observed are usually much better than those taken

from the two levels involved in an optical transition.

Finally, it is interesting to compare our result (28) with the one obtained from nuclear-Coulomb-excitation measurements. Collective nuclear-model calculations show that the transition probability for an electric-dipole transition between two nuclear levels I_i and I_f in the same rotational band is given by[16]

$$B(E2; I_i \rightarrow I_f) = (5/16\pi)\, e^2 Q_1^2 \Omega^2, \tag{29}$$

where B is the transition probability, $E2$ designates it as an electric-dipole transition, e is the electronic charge, Q_1 is the intrinsic nuclear quadrupole moment, and Ω is a matrix element connecting the two states.

The intrinsic quadrupole moment Q_1 is related to the quadrupole moment Q_0 in the nuclear ground state by[16]

$$Q_1 = Q_0 \frac{I(2I-1)}{(I+1)(2I+3)} \ . \tag{30}$$

It follows then that if one compares transition probabilities between states I_i and I_f for Gd^{155} and Gd^{157}, where I, I_i, and $I_f \equiv I$ are the same in both isotopes,

$$[B(E2)^{155}/B(E2)^{157}]^{1/2} = Q_0^{155}/Q_0^{157}. \tag{31}$$

From the tables of Alder *et al.*[16] we have

$$B(E2; \tfrac{5}{2} \rightarrow \tfrac{3}{2})^{155}/B(E2; \tfrac{5}{2} \rightarrow \tfrac{3}{2})^{157} = 3.3/3.5.$$

The square root of this ratio is 0.97, in very good agreement with our result.

*Present address: Department of Electrical Engineering, University of Southern California, Los Angeles, Calif. 90007.

[1]H. G. Kahle, V. Koch, J. Plamper, and W. Urban, J. Chem. Phys. 49, 2702 (1968).
[2]W. Urban, J. Chem. Phys. 49, 2703 (1968).
[3]J. Rosenthal, R. F. Riley, and U. Ranon, Phys. Rev. 177, 625 (1969).
[4]See Refs. 2 and 3 for discussion of the crystal-field parameters and further references.
[5]See, e.g., W. Low, in *Solid State Physics*, edited by F. Seitz and D. Turnbull (Academic, New York, 1960), Suppl. 2.
[6]R. W. G. Wyckoff, *Crystal Structures* (Interscience, New York, 1965), Vol. 3.
[7]M. T. Hutchings, Solid State Phys. 16, 227 (1965), and references therein.
[8]See, e.g., U. Ranon and J. S. Hyde, Phys. Rev. 141, 259 (1966).
[9]J. Rosenthal, Phys. Rev. 164, 363 (1967).
[10]B. Bleaney, Phil. Mag. 42, 441 (1951).
[11]J. M. Baker, G. M. Copland, and B. M. Wanklyn, J. Phys. C 2, 862 (1969).
[12]I. Lindgren, Arkiv Fysik 29, 553 (1965); see also V. S. Shirley, in *Hyperfine Structure and Nuclear Radiation*, edited by E. Matthias and D. A. Shirley (North-Holland, Amsterdam, 1968), table of nuclear moments.
[13]A. J. Freeman and R. E. Watson, Phys. Rev. 127, 2058 (1962).
[14]D. R. Speck, Phys. Rev. 101, 1725 (1956).
[15]N. I. Kaliteevskii, M. P. Chaika, I. Kh. Pacheva, and E. E. Fradkin, Zh. Eksperim. i Teor. Fiz. 37, 882 (1959) [Soviet Phys. JETP 10, 629 (1960)].
[16]K. Alder, A. Bohr, T. Huus, B. Mottelson, and A. Winther, Rev. Mod. Phys. 28, 432 (1956).

PHYSICAL REVIEW B VOLUME 3, NUMBER 7 1 APRIL 1971

Stopping Cross Sections for Fission Fragments of ^{252}Cf by Gold, Silver, and Carbon†*

L. Bridwell and A. L. Walters, Jr.
Department of Physics, Murray State University, Murray, Kentucky 42071
(Received 10 August 1970)

Using ^{252}Cf as a source of heavy ions, the stopping cross sections were determined for stopping media of gold, silver, and carbon. The dependence of stopping cross sections on the nuclear charge of the heavy ions was observed at approximately 1.3 cm/nsec. The results are in reasonable agreement with the theory by Lindhard. In some cases, better agreement can be obtained by using a formula published earlier by Bridwell and Moak.

I. INTRODUCTION

During the past few years technological developments, such as the transuranic heavy-ion accelerator, certain chemonuclear systems, and the fission electric cell have created the need for more information concerning energy loss by heavy ions in various types of stopping materials. The differential energy loss or the stopping power of a material, is the amount of kinetic energy lost per unit path length and is given by the formula

$$-\frac{dE}{dx} = n\sigma, \tag{1}$$